Heliyon 10 (2024) e30418

Contents lists available at ScienceDirect

Heliyon

journal homepage: www.cell.com/heliyon

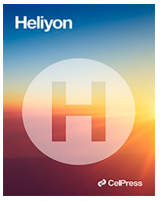

Research article

Electroacupuncture pretreatment alleviates rats cerebral ischemia-reperfusion injury by inhibiting ferroptosis

Tao Ye [a,1], Ning Zhang [b,1], Anbang Zhang [c], Xiuqi Sun [c], Bo Pang [c], Xuemei Wu [a,*]

[a] Department of Rehabilitation, The First Affiliated Hospital of Guizhou University of Traditional Chinese Medicine, Guiyang, 550001, Guizhou, China
[b] Department of Pharmacy, The First Affiliated Hospital of Guizhou University of Traditional Chinese Medicine, Guiyang, 550001, Guizhou, China
[c] Department of Neurology, The First Affiliated Hospital of Guizhou University of Traditional Chinese Medicine, Guiyang, 550001, Guizhou, China

ARTICLE INFO

Keywords:
Cerebral ischemia-reperfusion injury
Electroacupuncture pretreatment
Ferroptosis
Oxidative stress

ABSTRACT

Objective: To explore the preventive effect of electroacupuncture pretreatment on stroke in rats by inhibiting ferroptosis and oxidative stress.
Methods: Rats were randomly assigned to the sham, middle cerebral artery occlusion/reperfusion (MCAO/R), MCAO/R + EP, MCAO/R + EP + erastin, and MCAO/R + EP + ferrostatin 1 groups. Daily electroacupuncture was performed 2 weeks before establishing the MCAO/R model utilizing the modified Zea Longa suture method. Rats were sacrificed 1 day after reperfusion, and brain tissues were collected. They were prepared for hematoxylin and eosin staining, prussian blue staining, transmission electron microscope. Measurement of total iron levels using a commercial kit, detection of malondialdehyde (MDA) and superoxide dismutase (SOD) levels by ELISA, and examination of 15-lox2, GPX4, SLC7A11, ACSL4, and TFR1 by western blotting.
Results: Compared with sham rats, cerebral infarction size was dramatically larger in MCAO/R rats. Moreover, the MCAO/R group displayed damaged mitochondria with a disarranged structure of cristae; free iron, total iron levels, and oxidative stress were significantly higher. Cerebral pathological lesions, oxidative stress, total iron levels, and protein levels of ACSL4, TFR1, and 15-lox2 were significantly reduced in the MCAO/R + EP and MCAO/R + EP + ferrostatin 1 groups, while the protective effect of electroacupuncture pretreatment on cerebral ischemia-reperfusion injury was inhibited by treatment with the ferroptosis activator erastin.
Conclusion: Electroacupuncture pretreatment can protect rats from cerebral ischemia-reperfusion injury by reducing the area of cerebral infarction and inhibiting ferroptosis and oxidative stress.

1. Introduction

Acute ischemic stroke is caused by a decrease in cerebral blood supply, has a high fatality rate, and frequently results in significant central nervous system (CNS) damage and sequelae [1]. The pathogenic process of cerebral ischemia-reperfusion damage (CIRI) is complex, involving energy metabolism abnormalities, oxidative stress injury, excitotoxicity, inflammatory response, and apoptosis[2], however, new study indicates that ferroptosis is also involved. Ferroptosis is a novel cell death mode that is different from apoptosis and necrosis in cell morphology and function. Ferroptosis is a unique oxidative stress-induced cell death pathway characterized by iron

* Corresponding author. No. 71 North Baoshan Road, Yunyan District, Guiyang, 550001, Guizhou, China.
E-mail address: zyyfykf@163.com (X. Wu).
[1] Tao Ye and Ning Zhang contributed equally to this work.

https://doi.org/10.1016/j.heliyon.2024.e30418
Received 6 November 2023; Received in revised form 24 April 2024; Accepted 25 April 2024
Available online 26 April 2024

overload and lipid peroxidation Ferroptosis is a regulated cell death process that was recently reported to exacerbate CIRI via mechanisms involving iron overload, excitotoxicity, antioxidant systems, and lipid peroxidation (LPO) [3]. Clinical trials and animal experimental studies of ischemic cerebrovascular illness have revealed that the brain is particularly susceptible to hypoxia and that local vascular constriction results in hypoxic environment adaptation [4].

Ischemic tolerance is an endogenous protective mechanism that prevents deadly ischemic injury by activating neuroprotective mechanisms through sublethal ischemia [5]. Preconditioning with sublethal stressors other than ischemia can also elicit these mechanisms in the brain. Electroacupuncture is a form of traditional Chinese medicine that blends acupuncture with modern electro-stimulation techniques. Previous research has demonstrated that electroacupuncture can help prevent middle cerebral artery occlusion/reperfusion (MCAO/R). Zhou et al. [6] found that 30 min of electroacupuncture pretreatment at Baihui 2 h before focal cerebral ischemia might produce ischemic tolerance in mouse models. The mechanism of electroacupuncture-induced ischemia tolerance may be directly related to autophagy suppression [7]. Other putative pathways by which electroacupuncture pretreatment protects against ischemia, however, remain unknown.

Ferroptosis, a recently identified type of programmed cell death, is characterized by the accumulation of lipid reactive oxygen species (ROS) produced by antioxidant capacity depletion. The main cause of ferroptosis is intracellular iron excess [8]. Dixon et al. proposed ferroptosis in 2012, describing it as an intracellular iron-dependent programmed cell death triggered by the small-molecule complex erastin. Erastin inhibits cystine import, resulting in glutathione depletion and decreased glutathione peroxidase 4 (GPX4) antioxidant activity. As a result of the uneven intracellular redox and accumulation of lipid peroxidation products, cell death occurs [9]. Iron overload in the ischemic brain is thought to be mainly due to the blocking of iron outflow and the increase of iron import. In mammals, ferroportin1 (FPN1) is the only cellular iron exporter [10]. By regulating FPN1 expression post-translationally, increased brain expression of hepcidin following ischemia may modulate iron output [11]. Reactive oxygen species (ROS) are produced by iron overload via the Fenton reaction [12]. Following cerebral ischemia, lipoxygenase is strongly expressed, and lipoxygenase inhibitors can prevent brain damage by preventing ferroptosis.

Brain ischemia-induced ROS have the capacity to interact with lipid membrane polyunsaturated fatty acids (PUFAs) to generate lipid peroxidation since there are multiple pathogenic reasons for ischemia-reperfusion damage. Moreover, treating one condition alone has significant limitations because ferroptosis induction also depends on glutathione (GSH) depletion and nicotinamide adenine dinucleotide phosphate (NADPH)-dependent lipid peroxidation. Unexpected outcomes may occur if treatment is directed at numerous causal variables. Electroacupuncture, as an essential alternative and complementary medicine, has benefits in the treatment of various disorders. As a result, we used electroacupuncture pretreatment and established an MCAO/reperfusion model in rats to investigate the effect and mechanism of electroacupuncture pretreatment on ferroptosis and oxidative stress in ischemia-reperfusion injury, with the hope of providing a theoretical and experimental foundation for the clinical application of electroacupuncture in CIRI disease.

2. Materials and methods

2.1. Experimental rats

All animals were kept in a pathogen-free environment and fed ad libitum. The Ethics Committee of Jiangxi Zhonghong Boyuan Biotechnology Co., Ltd. approved the procedures for the care and use of animals (approval number: 2021052803) and abided by all applicable institutions and government regulations on the ethical use of animals. A total of 30 male Sprague-Dawley rats with specific pathogen-free levels were obtained from Human SJA Laboratory Animal Co., Ltd. (Human, SCXK 2019-0004). They were habituated to a standard environment with a temperature of 20–26 °C and humidity of 40–70 %.

2.2. Reagents and instruments

Ferrostatin 1 (HY100579) and erastin (HY15763) were from MedChemExpress; Rat Superoxide Dismutase (SOD) ELISA Kit (MM-0386R2) and Rat Malondialdehyde (MDA) ELISA Kit (MM-0385R2) were from Meimian, Wuhan, China; PVDF membranes (IPVH00010) were from Millipore; Hypersensitive luminescent solution (RJ239676) was from ThermoFisher; Mouse monoclonal anti-actin antibody (TA-09, 1/2000) and peroxidase-conjugated goat anti-rabbit IgG (H + L) antibody (ZB-2301, 1/2000) were from ZSGB-Bio, Beijing, China; Rabbit anti-15-lox2 antibody (bs-6335R, 1/500) was from Bioss; Rabbit anti-GPX4 antibody (df6701, 1/500), rabbit anti-ACSL4 antibody (df12141, 1/500) and rabbit anti-TFR1 antibody (af5343, 1/500) were from Affinify; and Rabbit anti-XCT (SLC7A11) antibody (ab175186, 1/500) was from Abcam.

The vertical electrophoresis apparatus (DYY-6C) and microplate reader (WD-2102B) were from LIUYI, Beijing; the hemiDocTM XRS + System was from Bio-Rad Laboratories; the fully automated vibrating blade microtome (2235) was from Leica, and a light microscope (BX43) was from Olympus.

2.3. MCAO/R model

Rats were randomly assigned to the sham(n = 6), MCAO/R(n = 6), MCAO/R + EP(n = 6), MCAO/R + EP + erastin(n = 6), and MCAO/R + EP + ferrostatin 1 groups (n = 6). Briefly, 1.5 % sodium pentobarbital was used to anesthetize the rats at 45 mg/kg via intraperitoneal administration. After shaving and disinfection, a longitudinal incision was made along the midline of the neck, while the sternocleidomastoid muscle and neck muscle group were bluntly separated to expose the right common carotid artery. Subsequently, ligation was performed on the proximal end of the right common carotid artery as well as the external carotid artery, with the

internal carotid artery clamped. A 4-0 nylon monofilament was inserted into the right external carotid artery and advanced to block the middle cerebral artery 1 h before the filament was withdrawn. The incision was sutured and the rats were transferred to the cage after awakening.

2.4. Electroacupuncture pretreatment and medication

After intraperitoneal injection of 1.5 % sodium pentobarbital for anesthesia, electroacupuncture pretreatment using the needle at 0.25 mm × 25 mm at Baihui with a depth of 5 mm and frequency of 2 Hz/15 Hz was performed using an electroacupuncture apparatus (Model G 6805-2 A, SMIF, Shanghai). The negative and positive poles were connected to the needle handle and root of the right ear, respectively. During the electroacupuncture pre-treatment process, the surrounding environment was kept quiet. It was performed daily for six days per week for a total of two weeks.

Rats in the MCAO/R + EP + erastin and MCAO/R + EP + ferrostatin 1 groups were anesthetized and placed on a stereotaxic apparatus. A total of 10 μL of 10 μmol/L erastin and 0.48 mg/mL ferrostatin 1 was injected 1.08 mm below the coronal suture that was 2 mm away from the midline of the brain using a microinjector in rats of the MCAO/R + EP + erastin group and MCAO/R + EP + ferrostatin 1 group. Following a 10-min injection at 0.5 μL/min, the micro-injection pump stays for 5 min to disperse the agent, then continues to inject for an additional 10 min. Within 4 min, the micro-syringe is carefully removed to minimize agent backflow.

2.5. TTC staining

Rats were sacrificed and brain tissue was made into 2 mm sections. Brain slices were immediately put into a 24-well plate, incubated with 2,3,5-triphenyltetrazole chloride (TTC, 2 %) at 37 °C for 15 min, and then fixed in 4 % paraformaldehyde. Slices show a rose-red normal area and a white infarct area, and the brain slices of each rat are arranged neatly and photographed. Image analysis was performed with Image J software, and the infarct area and total area of each slice were measured.The sum of the infarct area from each section was equal to the total infarct volume. To minimize the error induced by edema, the infarct volume was calculated as follows: Infarct volume = contralateral hemisphere region - non-infarcted region in the ipsilateral hemisphere. Infarct percentage (%) = infarct volume/contralateral hemisphere volume × 100.

2.6. HE staining

After collecting the tissues from each animal, the tissues were rinsed with water for 2 h. After dehydration using different concentrations of ethanol, the tissues were dehydrated with xylene until transparent, embedded for 1 h, and sliced. Subsequently, the slides were roasted, dewaxed, hydrated, immersed in distilled water, and stained in hematoxylin aqueous solution for 3 min, followed by differentiation with hydrochloric acid ethanol differentiation solution for 15 s. After being slightly washed with water and blue-returning solution for 15 s, the slides were rinsed with water and stained with eosin for 3 min. Images were obtained using an inverted microscope (Zeiss, Oberkochen, Germany).

2.7. Prussian blue staining

After 24 h of reperfusion, intracellular iron deposition was analyzed through Koeppen's Perls'Prussian blue staining. The brain tissue was processed into 10 μm-thick paraffin slices, then xylene I and xylene II were applied and left for 15 s each. Then, the sections were hydrated for 1 min each with varying grades of ethanol: 100 %, 95 %, 85 %, 75 %, and 70 %. Afterwards, Perls' staining solution (80 mL, 20 % HCl and 80 mL, 10 % potassium ferrocyanide) was employed to soak the sections for 20–30 min and distilled water was applied to rinse them for 3 times. After Eosin staining for 1 min, the sections were set in 80 %, 85 %, 90 % and 100 % ethanol solution for rapid gradient dehydration. 5 s later, the slices were fastened with xylene, then sealed with neutral resin.

2.8. Transmission electron microscope

A small piece of brain tissue (about 1 mm^3) was cut from the brain tissue of rats and fixed in 2.5 % glutaraldehyde at 4 °C for 2–4 h. The tissues were rinsed with 0.1 M phosphoric-acid bleach solution 3 times, 15 min each time, and then fixed in a 1 % osmic acid refrigerator at 4 °C for 2 h. The fixed tissues were dehydrated successively in 30 %, 50 %, 70 %, 80 %, 95 %, 100 %, and 100 % alcohol for 15 min each time, and 100 % propylene oxide 3 times for 5 min each time. After dehydration, propylene oxide + embedding solution (1:1) at 37 °C for 2 h, propylene oxide + embedding solution (1:2) at 37 °C for 5 h, pure embedding solution at 37 °C oven overnight. Then, the embedded plate was placed in an oven at 60 °C for 48 h. After the resin was completely polymerized, the embedded block was taken out-for use. After rough repair, the resin block was positioned in the semi-thin section of the ultra-thin slicer (Leica UC7, Germany). Finally, they were stained with 2 % uranium acetate saturated alcohol solution for 8 min. Then, the following steps were carried out: 70 % alcohol cleaning 3 times, ultrapure water cleaning 3 times, Staining with 2.7 % lead citrate solution for 8min, Cleaning 3 times with ultra-pure water, and blotting slightly with filter paper. The stained sections were observed and photographed under the transmission electron microscope (JEM-1230, Japan).

2.9. ELISA

The levels of Total iron levels, MDA, and SOD in rat brain tissue were evaluated by ELISA test. Homogenize rat brain tissue with cold physiological saline, centrifuge at 4 °C at 4000 rpm for 15 min, and collect supernatant. According to the manufacturer's instructions. The samples were measured in duplicate. The reading of each sample was normalized to protein concentration.

2.10. Western blotting

Proteins were isolated with lysis buffer and quantified using the bicinchoninic acid assay method (pc0020, Solarbio, Beijing, China). Proteins were separated by SDS-PAGE at a concentration of 12 %, followed by transfer of proteins to a PVDF membranes (IPVH00010, Millipore, Massachusetts, USA). After blocking, the membranes were incubated with primary antibodies at 4 °C for 12 h, washed, and incubated with secondary antibody (1:2000, 7074, CST, USA) for 90 min. Finally, the protein levels were quantified by analyzing the bands using Image J software.

2.11. Statistical analysis

Data are presented as mean ± standard deviation and were analyzed by one-way ANOVA using the S–N–K test. Statistical significance was determined when the value of P was lower than 0.05.

3. Results

3.1. Effects of electroacupuncture pretreatment, ferroptosis agonist erastin, and ferroptosis inhibitor ferrostatin 1 on cerebral infarction

Compared with the sham operation group, the infarct size was significantly larger in MCAO/R rats ($P < 0.05$) and dramatically reduced in the MCAO/R + EP group ($P < 0.05$). Moreover, erastin treatment aggravated cerebral infarction, while the opposite result was achieved with ferrostatin 1 treatment ($P < 0.05$) (Fig. 1).

3.2. Effects of electroacupuncture pretreatment, ferroptosis agonist erastin, and ferroptosis inhibitor ferrostatin 1 on pathological lesions of CIRI

Rat brain tissues were collected after sacrifice and stained with hematoxylin and eosin. No obvious pathological changes were observed in the sham group. At 24 h after MCAO, neuronal pyknosis and dissolution, cell body shrinkage, swelling of neurons and glial cells in the surrounding tissues of the infarction area, and enlargement of nerve cells and perivascular space were observed, which were

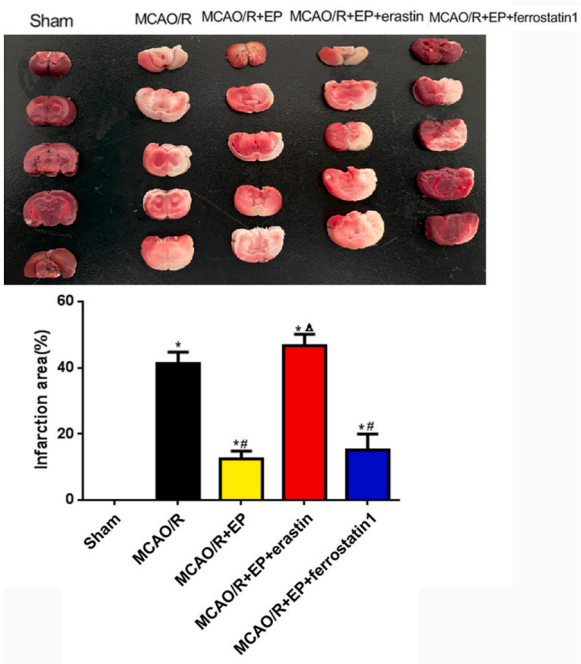

Fig. 1. Impact of electroacupuncture pretreatment (EP), ferroptosis agonist erastin, and ferroptosis inhibitor ferrostatin 1 on cerebral infarction. *$P < 0.05$ vs. sham group, $^{\#}P < 0.05$ vs. MCAO/R, $^{\Delta}P<0.05$ vs. MCAO/R + EP.

milder in the MCAO/R + EP group and MCAO/R + EP + ferrostatin 1 group, but more aggravated in the MCAO/R + EP + erastin group (Fig. 2).

3.3. Regulatory effects of electroacupuncture pretreatment, ferroptosis agonist erastin, and ferroptosis inhibitor ferrostatin 1 on free iron levels

Prussian blue staining further showed that, relative to the sham group, the deposition of free iron in brain tissues was significantly increased in the MCAO/R group ($P < 0.05$). Compared with the MCAO/R group, free iron levels were lower in the EP and MCAO/R + EP + ferrostatin 1 groups ($P < 0.05$) (Fig. 3).

3.4. Regulatory effects of electroacupuncture pretreatment, ferroptosis agonist erastin, and ferroptosis inhibitor ferrostatin 1 on mitochondrial

Compared with the sham group,the MCAO/R group displayed damaged mitochondria with a disarranged structure of cristae ($P < 0.05$), significantly restored the damaged cristae structure in the EP group ($P < 0.05$), indicating that EP is at least partially responsible for the maintenance of mitochondrial quality. (Fig. 4).

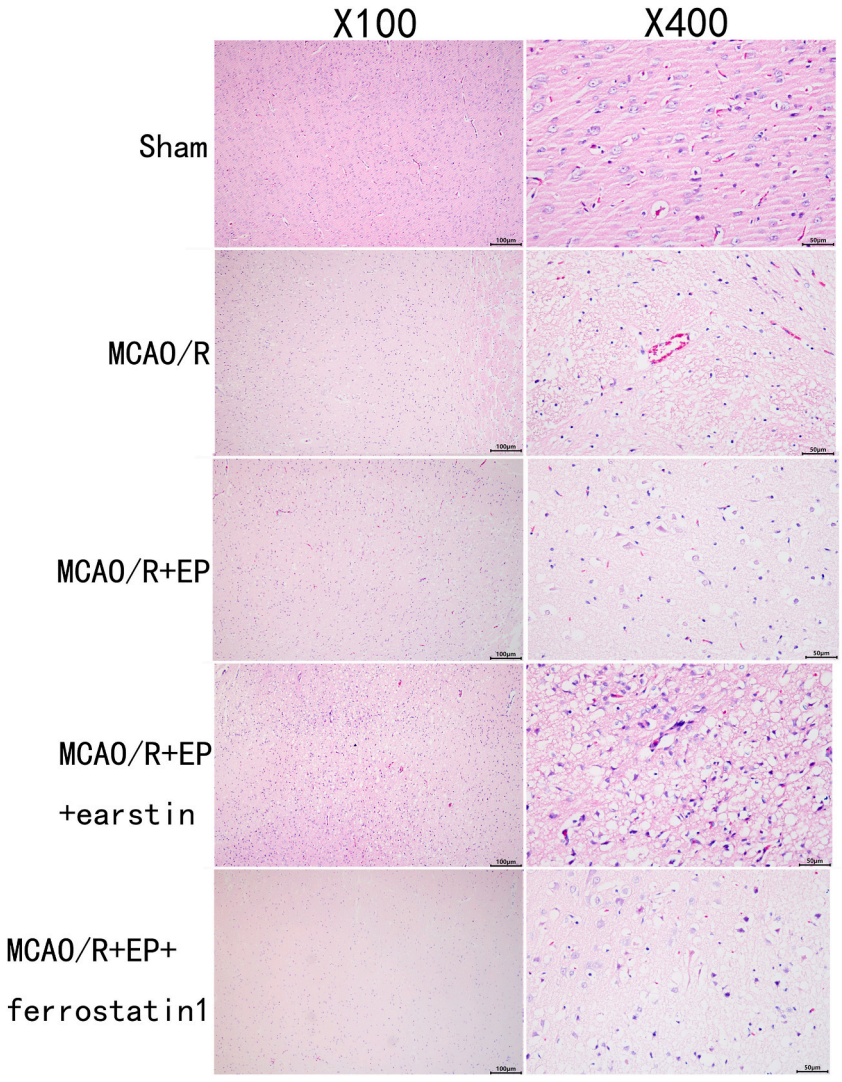

Fig. 2. Hematoxylin and eosin staining of rat brain tissues (× 100 and × 400). electroacupuncture pretreatment.

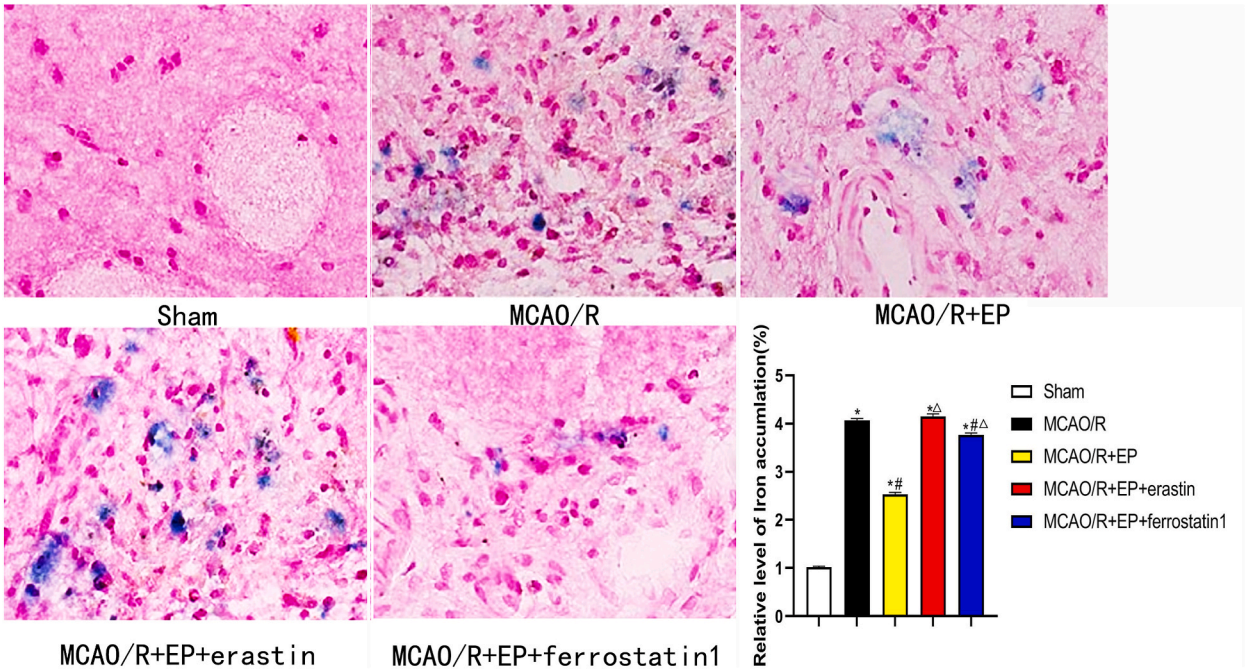

Fig. 3. Prussian blue staining analyzed the deposition of free iron in rat brain tissues (magnification: 200 ×). $^{*}P < 0.05$ vs. sham group, $^{\#}P < 0.05$ vs. MCAO/R, $^{\Delta}P<0.05$ vs. MCAO/R + EP.

3.5. Regulatory effects of electroacupuncture pretreatment, ferroptosis agonist erastin, and ferroptosis inhibitor ferrostatin 1 on total iron levels, MDA, and SOD levels

Compared with the sham group, total iron levels and MDA levels were elevated, while SOD levels were lower in the MCAO/R and MCAO/R + EP + erastin groups ($P < 0.05$). Significantly lower levels of total iron levels and MDA and higher SOD levels were detected in the MCAO/R + EP and MCAO/R + EP + ferrostatin 1 groups ($P < 0.05$) [Fig. 5(A-C)].

3.6. Regulatory effects of electroacupuncture pretreatment, ferroptosis agonist erastin, and ferroptosis inhibitor ferrostatin 1 on protein levels of GPX4, SLC7A11, ACSL4, TFR1 and 15-lox2

Compared with the sham group, we detected significantly downregulated GPX4 and SLC7A11 and upregulated ACSL4, TFR1, and 15-lox2 ($P < 0.05$). Notably, electroacupuncture pretreatment and ferrostatin 1 significantly upregulated GPX4 and SLC7A11, and downregulated ACSL4, TFR1, and 15-lox2 (Fig. 6).

4. Discussion

Ischemic stroke is becoming more common in middle-aged and older people. In ischemic stroke patients, the use of thrombolytic medicines to restore blood reperfusion is preferred. However, antithrombotic medications are ineffective, and treating secondary damage caused by thrombolysis-induced reperfusion is difficult in practical practice [13]. Electroacupuncture is a prevalent method in traditional Chinese medicine, where the intensity and frequency are quantified and modifiable [14]. Baihui (GV20) is a Du meridian acupoint that is useful for increasing Yang and replenishing Qi, arousing the brain and helping the orifices, dredging collaterals, and regulating Qi [15]. Baihui acupuncture has been proven to significantly reduce ischemic brain damage [16,17]. Previous research has shown that electroacupuncture prevents ischemia-reperfusion injury during the pre-ischemia, ischemia, and reperfusion stages [18,19]. The results of TTC staining indicated that the infarction size was substantially higher in MCAO/R rats, which was confirmed by pathological investigation. Notably, ischemic brain lesions were dramatically improved in rats pretreated with electroacupuncture, indicating that electroacupuncture has an excellent preventive effect against CIRI.

Dixon et al. were the first to describe ferroptosis in 2012. It is an iron-dependent cell death mechanism caused by the accumulation of lipid peroxides and relevant metabolites in the plasma membrane and the depletion of polyunsaturated fatty acids [20]. Iron overload and a huge accumulation of lipid peroxides in cells define ferroptosis [21]. Cells accumulate iron after responding to stimuli. Excess iron ions eventually cause membrane lipid peroxidation via the Fenton reaction, resulting in mitochondrial damage, decreased function, and, eventually, cell death [22]. Furthermore, in both clinical and ischemic stroke models, it leads to neuronal injury upon reperfusion [23,24]. A prior study found that using a ferroptosis inhibitor significantly reduces CIRI [25]. Our study found that, when compared to MCAO/R rats treated with electroacupuncture, those treated with the ferroptosis agonist had larger infarctions and more

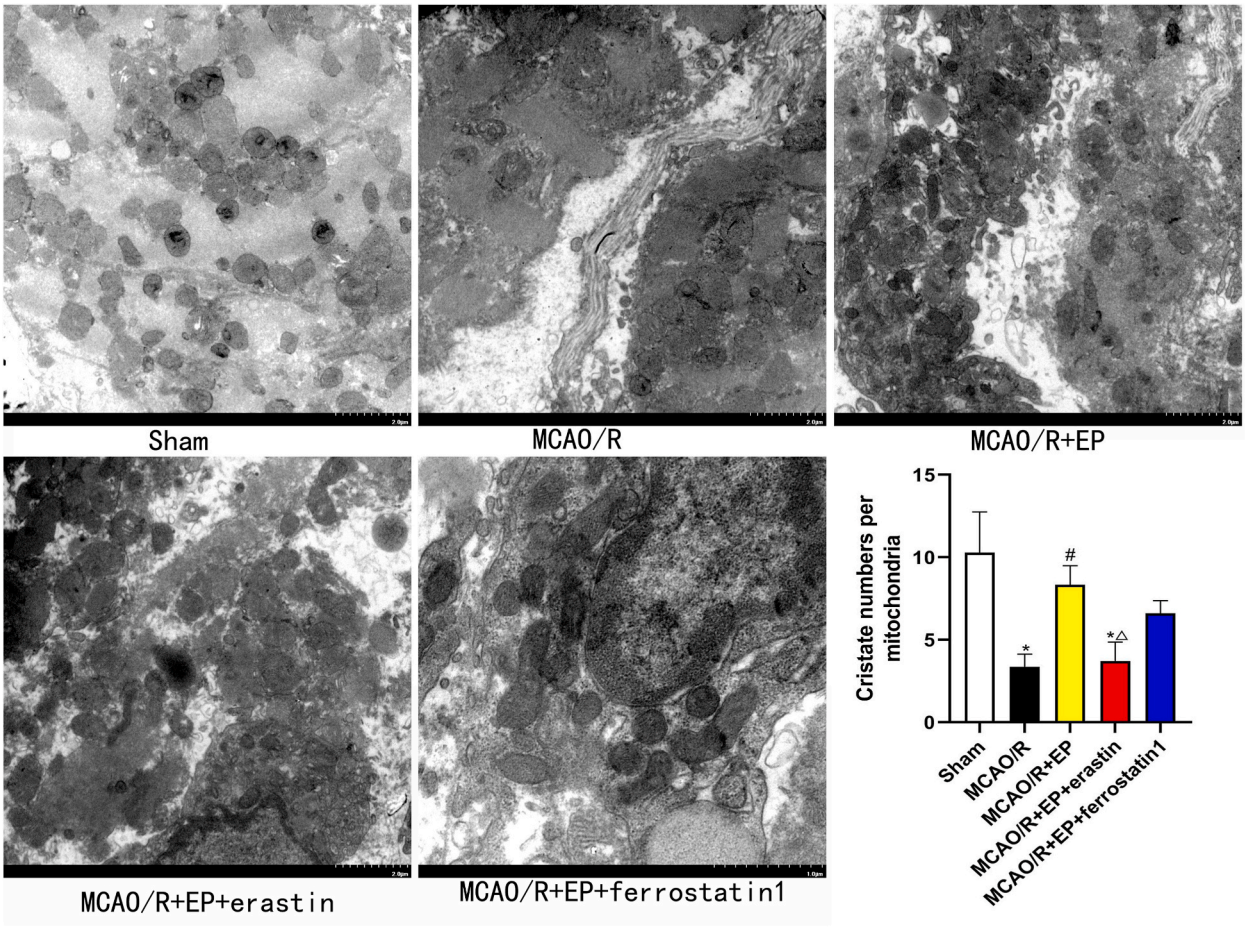

Fig. 4. Representative images of the mitochondria in rat brain tissues under the TEM images. Bar graphs depict the cristae numbers per mitochondria in rat brain tissues. Scale bars, 2.0 μm.

severe pathological lesions in the brain, whereas there were no significant differences between those treated with electroacupuncture and the ferroptosis inhibitor. It has also been proposed that pretreatment with electroacupuncture may decrease ferroptosis, although the addition of a ferroptosis inhibitor did not achieve a dual effect. Ferroptosis is connected to oxidative stress caused by Fe^{3+} [26]. We investigated iron and oxidative stress indicators in CIRI mice in this study. Total iron and MDA levels in MCAO/R rats increased considerably, while SOD levels declined significantly. The MCAO/R + EP and MCAO/R + EP + ferrostatin 1 groups showed the opposite tendency, indicating that electroacupuncture pretreatment could reduce ferroptosis and oxidative stress.

SLC7A11 is an essential protein in the cystine/glutamate transport pathway. SLC7A11 deficiency reduces cystine-dependent GPX4 activity and antioxidant ability, eventually resulting in ferroptosis [27,28]. TFR1 is a critical intracellular regulator of iron transport that regulates iron uptake and cell development [29]. Erastin, a ferroptosis agonist, has been shown to enhance ferroptosis in mouse lung fibroblasts by upregulating TFR1 [30]. According to reports, arachidonic acid and adrenal acid are catalyzed by arachidonic acid CoA and adrenoyl CoA, respectively. The manufacturing of membrane phospholipids is aided further, causing long-chain phospholipids to be localized on the cell membrane. Polyunsaturated fatty acids oxidize quickly, leading to increased lipid ROS, mitochondrial shrinkage, and cellular ferroptosis [31]. ACSL4, LPCTA3, and 15-lox generate unsaturated fatty acids such as arachidonic acid (AA) or adrenoyl (AdA), which enhance the generation of lipid ROS. As a result, deleting or inhibiting ACSL4, LPCTA3, and 15-lox can prevent ferroptosis [32]. To further explore the correlation between electroacupuncture pretreatment and ferroptosis, protein levels of GPX4, SLC7A11, ACSL4, TFR1, and 15-lox2 were measured. Downregulated GPX4 and SLC7A11, and upregulated ACSL4, TFR1, and 15-lox2, were detected in rats in the MCAO/R group, which were reversed in the MCAO/R + EP and MCAO/R + EP + ferrostatin 1 groups, but further aggravated by electroacupuncture combined with erastin treatment. We believed that electroacupuncture pretreatment alleviated CIRI by repressing ferroptosis.

In conclusion, electroacupuncture pretreatment can resist ischemia-reperfusion injury by reducing the area of cerebral infarction, alleviating tissue damage, and inhibiting ferroptosis and oxidative stress.

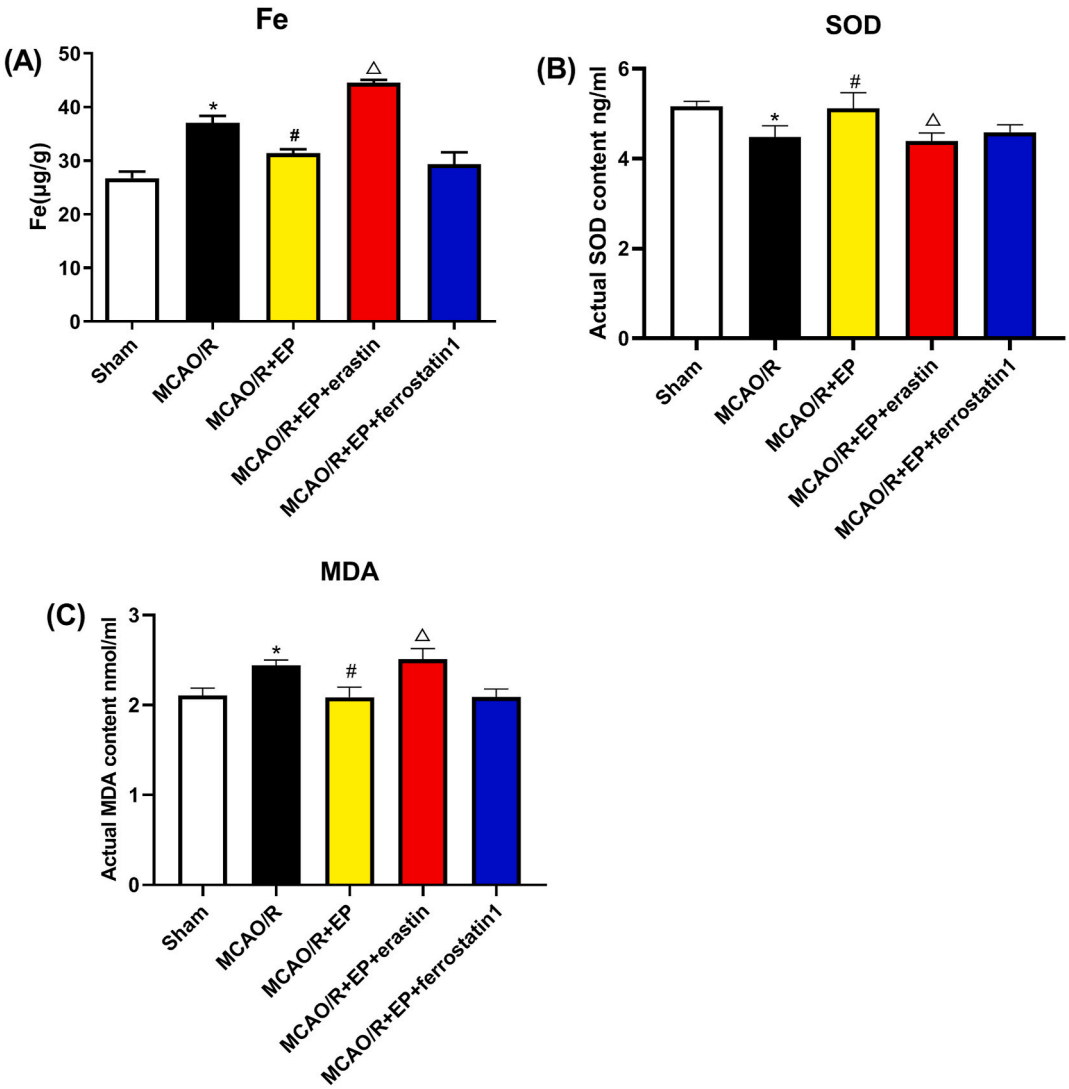

Fig. 5. (A–C) Total iron levels(A), malondialdehyde (MDA) (B) and superoxide dismutase (SOD) levels (C) in rat brain tissues. $^{*}P < 0.05$ vs. sham group, $^{\#}P < 0.05$ vs. MCAO/R, $^{\Delta}P<0.05$ vs. MCAO/R + EP.

Ethical statement

This research plan was reviewed and approved by The Ethics Committee of Jiangxi Zhonghong Boyuan Biotechnology Co., Ltd. approved the procedures for the care and use of animals (approval number: 2021052803).

Funding

This work was supported by (1) the National Natural Science Foundation of China (No. 82060896), (2) Guizhou Province Basic Research Project (No. QianKeHeJiChu - ZK[2021]General 505); (3) Science and Technology Support Program of Guizhou Province (No. QianKeHeZhiCheng[2021]General 019); (4) Youth Science and Technology Talent Growth Project of the Guizhou Provincial Department of Education (No. QianJiaoHe KY Zi[2021]210); (5) Science and Technology Fund Project of the Guizhou Provincial Health Commission (No. gzwkj2021-072); (6) Research Project of Traditional Chinese Medicine and Ethnic Medicine Science and Technology of the Guizhou Provincial Administration of Traditional Chinese Medicine (No. QZYY-2021-015).

CRediT authorship contribution statement

Tao Ye: Writing – review & editing, Writing – original draft, Visualization, Formal analysis, Data curation, Conceptualization. **Ning Zhang:** Writing – review & editing, Writing – original draft, Visualization, Formal analysis, Data curation, Conceptualization. **Anbang**

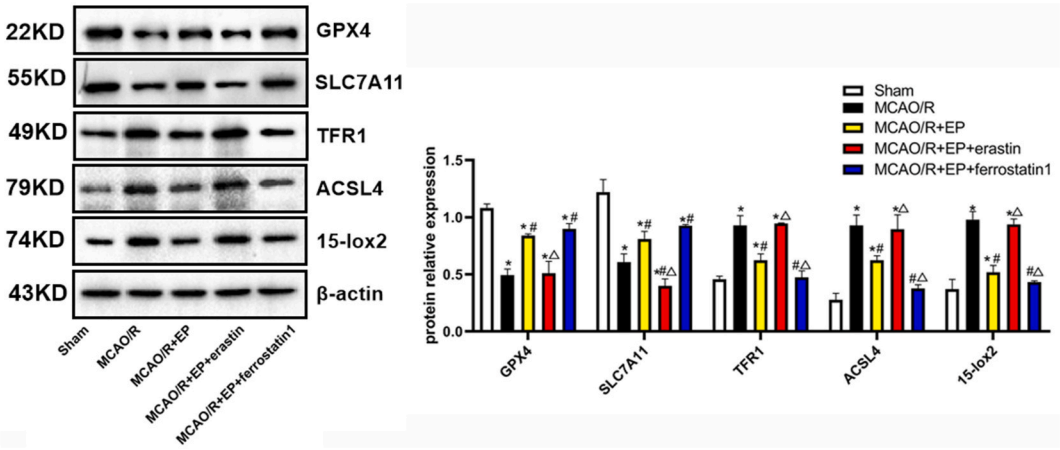

Fig. 6. Protein levels of GPX4, SLC7A11, ACSL4, TFR1 and 15-lox2 in rat brain tissues(EP, electroacupuncture). $^{*}P < 0.05$ vs. sham group, $^{\#}P < 0.05$ vs. MCAO/R, $^{\Delta}P<0.05$ vs. MCAO/R + EP.

Zhang: Writing – original draft, Visualization, Formal analysis. **Xiuqi Sun:** Data curation, Conceptualization. **Bo Pang:** Writing – review & editing. **Xuemei Wu:** Writing – review & editing, Methodology, Conceptualization.

Declaration of competing interest

The authors declare that they have no known competing financial interests or personal relationships that could have appeared to influence the work reported in this paper.

Acknowledgement

We would like to acknowledge the reviewers for their helpful comments on this paper.

Appendix A. Supplementary data

Supplementary data to this article can be found online at https://doi.org/10.1016/j.heliyon.2024.e30418.

References

[1] M. Chen, D. Kronsteiner, J.A.R. Pfaff, et al., Emergency intubation during thrombectomy for acute ischemic stroke in patients under primary procedural sedation, Neurol. Res. Pract. 3 (1) (2021 May 17) 27. https://pubmed.ncbi.nlm.nih.gov/34001285/.
[2] JV 4th McClain, E.A. Chance, G.M. Polcha Jr., Letter to the editor regarding "Incidence of acute ischemic stroke and rate of mechanical thrombectomy during the COVID-19 Pandemic in a large tertiary care telemedicine network, World. Neurosurg. 142 (2020 Oct) 561–562. http://pubmed.ncbi.nlm.nih.gov/32987600/.
[3] L. Wang, C. Liu, L. Wang, et al., Astragaloside IV mitigates cerebral ischaemia-reperfusion injury via inhibition of P62/Keap1/Nrf2 pathway-mediated ferroptosis, Eur. J. Pharmacol. 944 (2023 Apr 5) 175516. https://pubmed.ncbi.nlm.nih.gov/36758783/.
[4] H. Atarashi, S. Uchiyama, H. Inoue, et al., Ischemic stroke, hemorrhage, and mortality in patients with non-valvular atrial fibrillation and renal dysfunction treated with rivaroxaban: sub-analysis of the EXPAND study, Heart Ves. 36 (9) (2021 Sep) 1410–1420. http://pubmed.ncbi.nlm.nih.gov/33728513/.
[5] J. Liu, Y. Gu, M. Guo, et al., Neuroprotective effects and mechanisms of ischemic/hypoxic preconditioning on neurological diseases, CNS Neurosci. Ther. 27 (8) (2021 Aug) 869–882. http://pubmed.ncbi.nlm.nih.gov/34237192/.
[6] H. Zhou, Z. Zhang, H. Wei, et al., Activation of STAT3 is involved in neuroprotection by electroacupuncture pretreatment via cannabinoid CB1 receptors in rats, Brain Res. 1529 (2013 Sep 5) 154–164. https://pubmed.ncbi.nlm.nih.gov/23880371/.
[7] Z.G. Mei, Y.G. Huang, Z.T. Feng, et al., Electroacupuncture ameliorates cerebral ischemia/reperfusion injury by suppressing autophagy via the SIRT1-FOXO1 signaling pathway, Aging (Albany NY) 12 (13) (2020 Jul 3) 13187–13205. https://pubmed.ncbi.nlm.nih.gov/32620714/.
[8] J. Ni, K. Chen, J. Zhang, et al., Inhibition of GPX4 or mTOR overcomes resistance to Lapatinib via promoting ferroptosis in NSCLC cells, Biochem. Biophys. Res. Commun. 567 (2021 Aug 27) 154–160. https://pubmed.ncbi.nlm.nih.gov/34157442/.
[9] S.J. Dixon, K.M. Lemberg, M.R. Lamprecht, et al., Ferroptosis: an iron-dependent form of nonapoptotic cell death, Cell 149 (5) (2012 May 25) 1060–1072. https://pubmed.ncbi.nlm.nih.gov/22632970/.
[10] S. Aschemeyer, B. Qiao, D. Stefanova, et al., Structure-function analysis of ferroportin defines the binding site and an alternative mechanism of action of hepcidin, Blood 131 (8) (2018 Feb 22) 899–910. https://pubmed.ncbi.nlm.nih.gov/29237594/.
[11] Y. Zhao, Z. Xin, N. Li, et al., Nano-liposomes of lycopene reduces ischemic brain damage in rodents by regulating iron metabolism, Free Radic. Biol. Med. 124 (2018 Aug 20) 1–11. https://pubmed.ncbi.nlm.nih.gov/29807160/.
[12] N. Yamada, T. Karasawa, T. Wakiya, et al., Iron overload as a risk factor for hepatic ischemia-reperfusion injury in liver transplantation: potential role of ferroptosis, Am. J. Transplant. 20 (6) (2020 Jun) 1606–1618. https://pubmed.ncbi.nlm.nih.gov/31909544/.
[13] S. Johnson, R. McCarthy, B. Fahy, et al., Development of an in vitro model of calcified cerebral emboli in acute ischemic stroke for mechanical thrombectomy evaluation, J. Neurointerventional Surg. 12 (10) (2020 Oct) 1002–1007. https://pubmed.ncbi.nlm.nih.gov/31900353/.

[14] Y. Tang, A. Xu, S. Shao, et al., Electroacupuncture ameliorates cognitive impairment by inhibiting the JNK signaling pathway in a mouse model of Alzheimer's disease, Front. Aging Neurosci. 12 (2020 Feb 6) 23. http://pubmed.ncbi.nlm.nih.gov/32116652/.
[15] J. Jittiwat, Laser acupuncture at GV20 improves brain damage and oxidative stress in animal model of focal ischemic stroke, J Acupunct Meridian Stud 10 (5) (2017 Oct) 324–330. https://pubmed.ncbi.nlm.nih.gov/29078967/.
[16] X. He, Y. Mo, W. Geng, et al., Role of Wnt/β-catenin in the tolerance to focal cerebral ischemia induced by electroacupuncture pretreatment, Neurochem. Int. 97 (2016 Jul) 124–132. https://pubmed.ncbi.nlm.nih.gov/26994873/.
[17] Y.S. Jung, S.W. Lee, J.H. Park, et al., Electroacupuncture preconditioning reduces ROS generation with NOX4 down-regulation and ameliorates blood-brain barrier disruption after ischemic stroke, J. Biomed. Sci. 23 (2016 Mar 8) 32. http://pubmed.ncbi.nlm.nih.gov/26952102/.
[18] H. Wang, S. Chen, Y. Zhang, et al., Electroacupuncture ameliorates neuronal injury by Pink1/Parkin-mediated mitophagy clearance in cerebral ischemia-reperfusion, Nitric Oxide 91 (2019 Oct 1) 23–34. https://pubmed.ncbi.nlm.nih.gov/31323277/.
[19] L. Liu, N.H. Wang, Q. Zhang, et al., Zhen Ci Yan Jiu, Micro-ribonucleic acids participate in electroacupuncture intervention-induced improvement of ischemic stroke 44 (9) (2019 Sept 25) 686–692. Chinese, http://pubmed.ncbi.nlm.nih.gov/31532140/.
[20] J.P.F. Angeli, R. Shah, D.A. Pratt, et al., Ferroptosis inhibition: mechanisms and opportunities, Trends Pharmacol. Sci. 38 (5) (2017 May) 489–498. http://pubmed.ncbi.nlm.nih.gov/28363764/.
[21] Z.J. Li, H.Q. Dai, X.W. Huang, et al., Artesunate synergizes with sorafenib to induce ferroptosis in hepatocellular carcinoma, Acta Pharmacol. Sin. 42 (2) (2021 Feb) 301–310. https://pubmed.ncbi.nlm.nih.gov/32699265/.
[22] L. Yang, Y. Liu, W. Zhang, et al., Ferroptosis-inhibitory difference between chebulagic acid and chebulinic acid indicates beneficial role of HHDP, Molecules 26 (14) (2021 Jul 15) 4300. https://pubmed.ncbi.nlm.nih.gov/34299576/.
[23] A. Dávalos, J. Castillo, J. Marrugat, et al., Body iron stores and early neurologic deterioration in acute cerebral infarction, Neurology 54 (8) (2000 Apr 25) 1568–1574. http://pubmed.ncbi.nlm.nih.gov/10762495/.
[24] X. Guan, Z. Li, S. Zhu, et al., Galangin attenuated cerebral ischemia-reperfusion injury by inhibition of ferroptosis through activating the SLC7A11/GPX4 axis in gerbils, Life Sci. 264 (2021 Jan 1) 118660. http://pubmed.ncbi.nlm.nih.gov/33127512/.
[25] Q.Z. Tuo, P. Lei, K.A. Jackman, et al., Tau-mediated iron export prevents ferroptotic damage after ischemic stroke, Mol. Psychiatr. 22 (11) (2017 Nov) 1520–1530. http://pubmed.ncbi.nlm.nih.gov/28886009/.
[26] Z. Xie, H. Hou, D. Luo, et al., ROS-dependent lipid peroxidation and reliant antioxidant ferroptosis-suppressor-protein 1 in rheumatoid arthritis: a covert clue for potential therapy, Inflammation 44 (1) (2021 Feb) 35–47. https://pubmed.ncbi.nlm.nih.gov/32920707/.
[27] Z. Guan, J. Chen, X. Li, et al., Tanshinone IIA induces ferroptosis in gastric cancer cells through p53-mediated SLC7A11 down-regulation, Biosci. Rep. 40 (8) (2020 Aug 28) 20201807. https://pubmed.ncbi.nlm.nih.gov/32776119/.
[28] X. Lang, M.D. Green, W. Wang, et al., Radiotherapy and immunotherapy promote tumoral lipid oxidation and ferroptosis via synergistic repression of SLC7A11, Cancer Discov. 9 (12) (2019 Dec) 1673–1685. https://pubmed.ncbi.nlm.nih.gov/31554642/.
[29] J. Lu, F. Xu, H. Lu, LncRNA PVT1 regulates ferroptosis through miR-214-mediated TFR1 and p53, Life Sci. 260 (2020 Nov 1) 118305. http://pubmed.ncbi.nlm.nih.gov/32827544/.
[30] C. Xiao, X. Fu, Y. Wang, et al., Transferrin receptor regulates malignancies and the stemness of hepatocellular carcinoma-derived cancer stem-like cells by affecting iron accumulation, PLoS One 15 (12) (2020 Dec 22) e0243812. http://pubmed.ncbi.nlm.nih.gov/33351833/.
[31] F.J. Xiao, Q.S. Ming, S. Miao, et al., Oleanolic acid inhibits cervical cancer Hela cell proliferation through modulation of the ACSL4 ferroptosis signaling pathway, Biochem. Biophys. Res. Commun. 545 (2021 Mar 19) 81–88. http://pubmed.ncbi.nlm.nih.gov/33548628/.
[32] S. Doll, B. Proneth, Y.Y. Tyurina, et al., ACSL4 dictates ferroptosis sensitivity by shaping cellular lipid composition, Nat. Chem. Biol. 13 (1) (2017 Jan) 91–98. http://pubmed.ncbi.nlm.nih.gov/27842070/.